ANALYSIS OF CATION VALENCES AND OXYGEN VACANCIES IN MAGNETORESISTIVE OXIDES BY ELECTRON ENERGY-LOSS SPECTROSCOPY

Z.L. WANG[a], J.S. YIN, Y. BERTA, J. ZHANG*

School of Material Science and Engineering, Georgia Institute of Technology, Atlanta, GA 30332-0245 USA. [a] e-mail: zhong.wang@mse.gatech.edu.
*Advanced Technology Materials, Inc., 7 Commerce Drive, Danbury, CT 06810; Currently at: Motorola, Inc., 3501 Ed Bluestein Boulevard, MD: K-10 Austin, TX 78721.

ABSTRACT

Magnetic oxides of (La,A)MnO_3 and (La,A)CoO_3 have two typical structural characteristics: cations with mixed valences and oxygen vacancies, which are required to balance the charge introduced by cation doping. The consequences introduced by each can be different, resulting in different properties. It is important to quantitatively determine the percentage of charges balanced by each, but this analysis is rather difficult particularly for thin films. This paper has demonstrated that electron energy-loss spectroscopy (EELS) can be an effective technique for analyzing Mn and Co magnetic oxides with the use of intensity ratio of white lines, leading to a new technique for quantifying oxygen vacancies in functional and smart materials.

INTRODUCTION

(La,A)MnO_3 and (La,A)CoO_3 (A = Ca, Sr, or Ba) are important magnetic oxides and their unique properties are determined by three structural characteristics [1]. First, the ferromagnetically ordered Mn-O (or Co-O) layers in the perovskite unit cell are isolated by non-magnetic La(A)-O layers, forming an intrinsic spin-coupling, which is the origin of the magnetic properties of the materials. Secondly, the electric conductivity of the materials is owing to the substituted divalent A^{2+}. The compounds with extreme values x = 0, 1 are neither ferromagnetic nor good electrical conductors. Only compounds with intermediate values of x are ferromagnetic. This is the most interesting characteristics of this type of materials. Finally, the co-existence of the cations with mixed valences and oxygen vacancies are the key factors for determining their unique properties.

The partial substitution of trivalent La^{3+} by divalent element A^{2+} is balanced by the conversion of Mn valence states from Mn^{3+} to Mn^{4+} (or Co^{3+} to Co^{4+} for Co) and the creation of oxygen vacancies. The ionic structure of $La_{1-x}A_xMnO_{3-y}$ is

$$La^{3+}_{1-x}\, A^{2+}_{x}\, Mn^{3+}_{1-x+2y}\, Mn^{4+}_{x-2y}\, O^{2-}_{3-y}\, V^{O}_{y} \qquad (1)$$

where V stands for the fraction of oxygen vacancies. Whenever a Mn^{3+} and a Mn^{4+} are on neighboring Mn sites, there exists the possibility of conductivity by electrons hopping from Mn^{3+} to Mn^{4+} with the assistance of an oxygen anion. That, this hopping current should be spin polarized was required for a process of two simultaneous electron hops (from Mn^{3+} onto O^{2-} and from O^{2-} onto Mn^{4+}, thus interchanging Mn^{4+} and Mn^{3+}), called *double exchange* [2]. Therefore, the residual charge introduced by cation substitution can be balanced by either valence conversion of the transition metal element or the creation of oxygen vacancies. If there is no valence conversion, the double exchange may not occur, leading to no or very minimal electrical conductivity. On the other hand, the increase of oxygen vacancies may increase the ionic conductivity.

From the analysis above, quantification of Mn valence and oxygen deficiency is the key for understanding the roles played by each in determination the properties and performance of the magnetic oxide. However, this analysis is a challenge to existing microscopy techniques particularly for thin films, because of the influence from the substrate surface, interface mismatch dislocations and defects in the film. A technique with high spatial resolution is required for this analysis. In this paper, electron energy-loss spectroscopy (EELS) in a transmission electron microscope (TEM) is introduced as a tool for quantifying the valence state of Mn (or Co) and the

Mat. Res. Soc. Symp. Proc. Vol. 494 © 1998 Materials Research Society

oxygen deficiency. The details of the technique are given, and its application in the two magnetic oxides containing Mn and Co, respectively, will be illustrated.

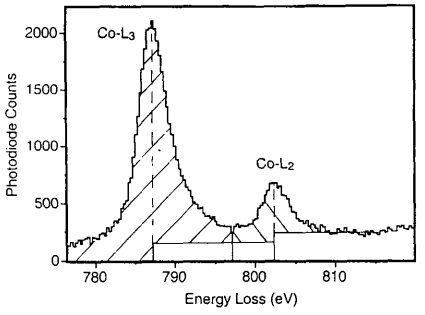

Figure 1. EELS spectrum acquired from $La_{0.67}Ca_{0.33}MnO_{3-y}$ showing the L_3 and L_2 white lines of the Mn ionization edges. The procedure of background subtraction is illustrated. This procedure must be followed consistently for all of the spectra.

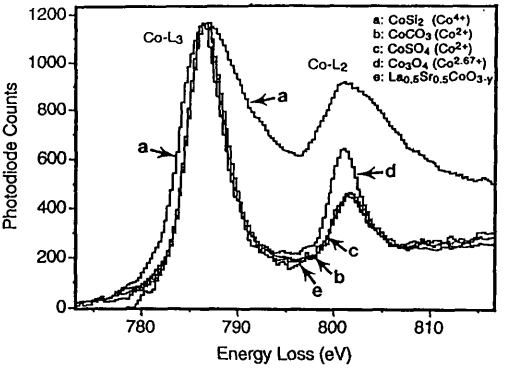

Figure 2. (a) A comparison of single-scattering EELS spectra of Co-$L_{2,3}$ ionization edges acquired from $CoSi_2$, $CoCO_3$, $CoSO_4$, Co_3O_4, and $La_{0.5}Sr_{0.5}CoO_{3-y}$. The spectra are displayed by normalizing the heights of the L_3 white lines.

EXPERIMENTAL APPROACH

In TEM, the interaction of the incident electron with the crystal electrons can generate various inelastic excitation processes [3]. One of the processes is the ionization of atomic inner shell bounded electrons, resulting in the ionization edge observed experimentally. In EELS, the L ionization edges of transition-metal, rare-earth and actinide compounds usually display sharp peaks at the near edge region (Figure 1). These threshold peaks are known as *white lines*. For transition metals with unoccupied 3d and 4d states, the white lines are observed. The unoccupied 3d states form a narrow energy band, the transition of a 2p state electron to the 3d levels leading to the formation of white lines observed experimentally. Thus, the atomic state changes from $2p^63d^{(m)}$ to $2p^53d^{(m+1)}$ after the excitation of a 2p electron, where m stands for the number of unoccupied 3d states. More specifically, the L_3 and L_2 lines are the transition of $2p^{3/2}$ -> $3d^{3/2}3d^{5/2}$ and $2p^{1/2}$ -> $3d^{3/2}$, respectively. EELS experiments have shown that the change in valence states of cations introduces significant changes in the ratio of the white lines, leading to the possibility of identifying the occupation number of 3d or 4d electrons (or cation valence states) using the measured white line intensities in EELS [4-6].

To establish the relationship between white line intensity and the number of unoccupied d electrons states, the white lines must be isolated from the background intensity. The EELS data must be processed first to remove the gain variation introduced by the detector channels and the multiple scattering effect via deconvolution. A low-loss valence spectrum and the corresponding core-shell ionization edge EELS spectrum were acquired from the same specimen region. The energy-loss spectrum was used to remove the multiple-inelastic-scattering effect in the core-loss region using the Fourier ratio technique, thus, the presented data are for single scattering. The background intensity was modeled by step functions in the threshold regions [5]. A straight line over a range of approximately 50 eV was fit to the background intensity immediately following each white line. This line was then extrapolated into the threshold region and set to zero at energies below that of the white-line maximum. The L_2 white line was further isolated by smoothly extrapolating the L_3 background intensity under the L_2 edge. For a case in which two white lines are not widely separated (Figure 1), a straight line is fit to the background immediately following the L_2 white line over a region of approximately 50 eV and is then extrapolated into the threshold region. This line was then modified into a double step of the same slop with onsets occurring at the

white-line maxima. The ratio of the step heights is chosen as 2:1 in accordance with the multiplicity of the initial states.

In the magnetic oxides with mixed valences and if the oxygen is ordered, the oxygen deficiency is directly correlated to the fraction of the mixed valences. From Eq. (1), the mean valence state of Mn is

$$\langle Mn \rangle_{VS} = 3 + x - 2y. \quad (2)$$

The $\langle Mn \rangle_{VS}$ can be determined using EELS as described above. Therefore, the content of oxygen vacancies y can be obtained. This is a new approach for studying oxide materials [7,8].

EXPERIMENTAL RESULTS

EELS analysis of valence state is usually carried out in reference to the spectra acquired from standard specimens with known cation valence states. If a series of EELS spectra are acquired from several standard specimens, an empirical plot of these data may serve as the reference for determining the valence state of the element present in a new compound. This is the basis of our analysis on the $La_{1-x}Sr_xCoO_{3-y}$ (LSCO) and $La_{1-x}Ca_xMnO_{3-y}$ (LCMO) magnetic oxides to be described below. The thin films were grown by metal-organic chemical vapor deposition (MOCVD) [9] and their crystal structures have been investigated previously [10].

$La_{0.5}Sr_{0.5}CoO_{3-y}$

$La_{1-x}Sr_xCoO_{3-y}$ has a perovskite-related structure, in which the mixed valence of the cations plays a vital role in determining the properties of the material. In the literature, Co has been believed to have valences 3+ and 4+ in this compound. The substitution of trivalent La^{3+} by divalent Sr^{2+} is balanced by creating oxygen vacancies as well as the conversion of Co^{3+} into Co^{4+} (or Co^{2+} into Co^{3+}). Thus, the ionic structure of $La_{1-x}Sr_xCoO_{3-y}$ can be either

$$La^{3+}_{1-x}\ Sr^{2+}_{x}\ Co_{1-x+2y}^{3+}\ Co_{x-2y}^{4+}\ O^{2-}_{3-y}\ V^{O}_{y} \quad (\text{for } y \le x/2) \quad (3)$$

or

$$La^{3+}_{1-x}\ Sr^{2+}_{x}\ Co_{1+x-2y}^{3+}\ Co_{2y-x}^{2+}\ O^{2-}_{3-y}\ V^{O}_{y} \quad (\text{for } x \le 2y) \quad (4)$$

depending on the concentration of the anion deficiency. In practice, the valence state of Co must be measured experimentally to determine the ionic configuration of the compound.

Figure 2 shows a comparison of the processed single-scattering EELS spectra of Co-$L_{2,3}$ ionization edges acquired from $CoSi_2$ (with Co^{4+}), Co_3O_4 (with $Co^{2.67+}$), $CoCO_3$ (with Co^{2+}) and $CoSO_4$ (with Co^{2+}) and $La_{0.5}Sr_{0.5}CoO_{3-y}$. The first four compounds are chosen as the standard specimens with known Co valences, and the last one is the specimen that we want to determine its Co valence state. It is apparent that the shape of $CoSi_2$ (with Co^{4+}) is dramatically different from the rest not only for its high L_2 edge but also for its broaden shape, simply because of its highest Co valence state. The other four specimens have the same line width and intensity except that Co_3O_4 (with $Co^{2.67+}$) has a higher L_2 edge, this is because of its larger Co valence. The two standard specimens showing the same shape of Co-$L_{2,3}$ edges have Co^{2+}. These spectra clearly establish the experimental basis of using the white line intensities for determination the Co valence in a new compound (Figure 3), which clearly shows that $I(L_3)/I(L_2)$ is very sensitive to the valence state of Co. From the empirical fitting curve, the valence of Co in $La_{0.5}Sr_{0.5}CoO_{3-y}$ can be determined from its $I(L_3)/I(L_2)$ value (= 5.05). The corresponding horizontal axis is approximately 1.93, which means the valence of Co in $La_{0.5}Sr_{0.5}CoO_{3-y}$ is 2+ with consideration of the experimental error. Therefore, the ionic structure of LSCO is described by Eq. (4) with $y = (x+1)/2 = 0.75$, which is

$$La^{3+}_{0.5}\ Sr^{2+}_{0.5}\ Co^{2+}O^{2-}_{2.25}\ V^{O}_{0.75}.$$

Chemical microanalysis using energy dispersive x-ray spectroscopy and EELS microanalysis and the in-situ EELS experiments [11] as well have confirmed this result. Based on this ionization formula, the crystal structure of a new rhombohedral phase of $La_{0.5}Sr_{0.5}CoO_{2.25}$ (or $La_8Sr_8Co_{16}O_{36}$) has been determined using the information provided by high-resolution

transmission electron microscopy and electron diffraction [8]. The unit cell is made out of two-types of fundamental modules and it is composed of a total of 8 modules. Each module is a c-axis stacking of the anion deficient $SrCoO_{3-z}$ and $LaCoO_{3-\delta}$ basic perovskite cells. The unit cell preserves the characteristics of perovskite framework and it is a superstructure induced by oxygen vacancies.

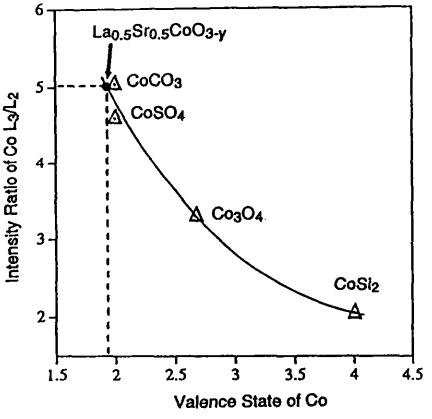

Figure 3. A plot of the intensity ratio of $I(L_3)/I(L_2)$ calculated from the spectra shown in Figure 2 for different compounds. The Co valence state in $La_{0.5}Sr_{0.5}CoO_{3-y}$ is obtained from the empirical fitting curve in reference to the known Co valences of the standard specimens.

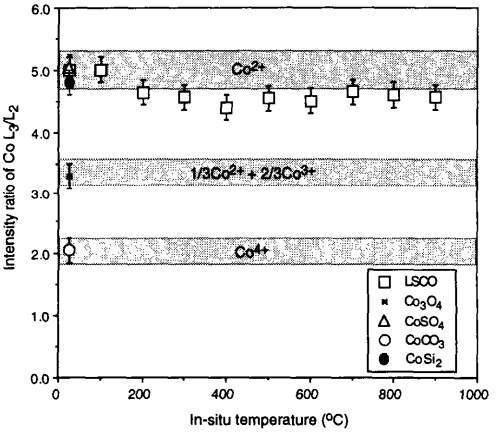

Figure 4. The intensity ratio of Co $I(L_3)/I(L_2)$ measured from LSCO as a function of the specimen temperature in TEM, showing the stability of the white line intensity. The specimen decomposes at 900 °C.

To check the reliability of the white line intensity for valence state measurement, the LSCO specimen was annealed in-situ from room temperature to 900 °C, until the film is decomposed to lower oxides. Figure 4 is a plot of the intensity ratio of Co $I(L_3)/I(L_2)$ as a function of the specimen temperature. It is striking that the intensity ratio of $I(L_3)/I(L_2)$ (= 4.5-4.9) remains almost constant up to 900 °C, above which the specimen started to decompose. At 1000 °C, the decomposed film is polycrystalline, but the valence state of Co is still 2+, proving the stability of white line ratio.

$La_{0.67}Ca_{0.33}MnO_{3-y}$

LCMO is an important group of materials that have been found to exhibits the colossal magnetoresistive effect [12,13]. To determined the average valence of Mn, Figure 5 shows a plot of the experimentally measured intensity ratio of white lines $I(L_3)/I(L_2)$ for several standard specimens with known Mn valences. It is apparent that the intensity ratio of $I(L_3)/I(L_2)$ strongly depends on the valence state of Mn. This curve serve as the standard for determining the valence state of Mn although it is non-linear. The $I(L_3)/I(L_2)$ ratio for LCMO is 2.05 - 2.17, thus, the average valence state of Mn is 3.2 to 3.5. Substituting this value into Eq. (3), yields $y \leq 0.065$, which is equivalent to less than 2.2 at.% of the oxygen content [7].

RELIABILITY AND ACCURACY OF THE MEASUREMENT

To determine the reliability and accuracy of the EELS measurement on valence state, a standard MnO_2 specimen was used in TEM to observe its in-situ reduction process as the specimen temperature is increased [16]. The chemical composition of the specimen is continuously determined using the integrated intensity of the ionization edges. A plot of composition, n_O/n_{Mn} and white line intensity, Mn $I(L_3)/I(L_2)$ is given in Figure 6, the shadowed bands indicate the white line ratios for Mn^{2+}, Mn^{3+} and Mn^{4+} as determined from the standard specimens of MnO, Mn_2O_3 and MnO_2, respectively. The reduction of MnO_2 occurs at 300 °C. As the specimen temperature increases, the O/Mn ratio drops and the $I(L_3)/I(L_2)$ ratio increases, which indicates the valence state conversion of Mn from 4+ to lower valence states. At T = 400 °C, the specimen contains the mixed valences of Mn^{4+}, Mn^{3+} and Mn^{2+}. As the temperature reaches 450 °C, the specimen is dominated by Mn^{2+} and the composition has O/Mn = 1.3 ± 0.5, slightly higher than that in MnO, which is consistent with the mixed valence of Mn cations and implies the uncompleted reduction of MnO_2.

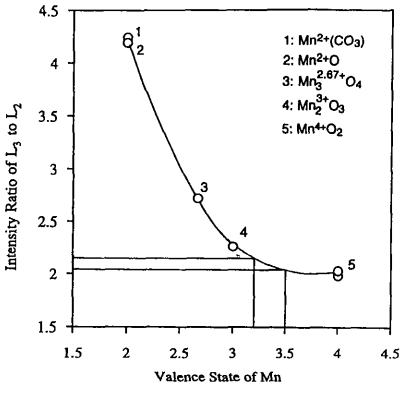

Figure 5. Plot of white line intensity ratio $I(L_3)/I(L_2)$ verses the valence state of Mn for several standard specimens of $MnFe_2O_4$, $MnCO_3$, MnO, Mn_2O_3 and MnO_2. A nominal fit of the experimental data is shown by a solid curve. The valence state of the LCMO film is obtained from the measured $I(L_3)/I(L_2)$ data.

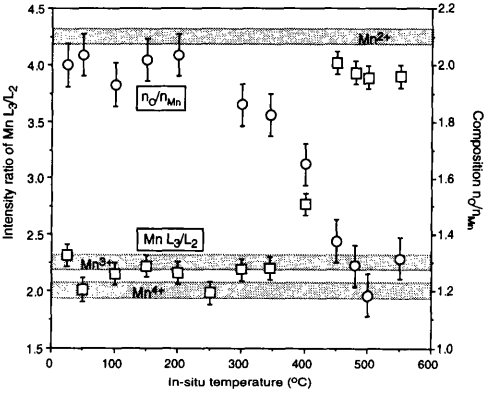

Figure 6. An overlapped plot of the white line intensity ratio of Mn $I(L_3)/I(L_2)$ and the corresponding chemical composition of n_O/n_{Mn} as a function of the in-situ temperature of the MnO_2 specimen based on EELS spectra, showing a continuously change in Mn valence state and oxygen composition.

DISCUSSIONS

It has been demonstrated by several authors [5,6] that the 3d and 4d electron occupations need to be determined with the use of the normalized white line intensity and the continuous spectrum at 50 to 100 eV above the edge threshold. This technique can give a linear fitting between the normalized white line intensity $[I(L_3) + I(L_2)]$ with the d state occupation, but it has two major shortcomings. One this linear curve is a good approximation for the entire occupation range from 0 to 10, but it is not a fair representation of the valence state if one is interested only in one element, such as Mn, whose 3d occupation can be 3, 2 or 1. The linear curve deviates largely from the experimental data if the 3d occupation is 1-3, leading to a significant inaccuracy in the measured result. With the use of the white line ratio $I(L_3)/I(L_2)$, the experimental data are steady and the difference between different valence state is significantly large, allowing more accurate determination of the valence state. The other one, in practical EELS, the intensity at a region 50-

100 eV above the edge threshold may be affected by the deconvolution and spectrum background subtraction procedures particularly when the noise level and gain variation are significant, resulting in a large error in the evaluation of the continuous part depending on specimen thickness. In contrast, the intensity ratio of $I(L_3)/I(L_2)$ has little dependence on the specimen thickness and its value is a steady number.

It has also been pointed out in the literature that the $I(L_3)/I(L_2)$ ratio is approximately the ratio of the electrons in the j = 5/2 and j = 3/2 states, thus, the white line intensity may be sensitive to the spin distribution [14,15]. From the EELS spectra of the four standard specimens, $CoCO_3$, $CoSO_4$, $CoSi_2$ and Co_3O_4 (with $Co^{2.67+}$) (see Figure 2), the former two with Co^{2+} show almost an identical Co-$L_{2,3}$ shape, while the last two with Co^{4+} and $Co^{2.67+}$ show a distinct difference in Co-L_2. A small difference in $I(L_3)/I(L_2)$ ratio between $CoCO_3$ and $CoSO_4$ in Figure 2 might be due to the spin effect, but this small fluctuation cannot significantly affect the measurement. This indicates that, at least in our case, the electron distribution in spin states, if any, plays a negligible role. The in-situ EELS analysis of valence conversion in transition metal oxides has shown the sensitivity and reliability of valence state measurement using white lines in Mn and Co oxides [16].

CONCLUSION

In this paper, electron energy-loss spectroscopy (EELS) in a transmission electron microscope has been demonstrated as a powerful technique for quantifying the valence conversion and oxygen deficiency in a magnetic oxide. This analysis is most adequate for thin films because of its high spatial resolution. With the use of the intensity ratio of white lines observed in EELS, the average valence of Mn or Co in a new material was determined in reference to the spectra acquired from standard specimens. The result was used to calculate the oxygen deficiency in the material, and this information is useful for constructing the anion deficient structure model.

ACKNOWLEDGMENT

This work was supported in part by NSF grant DMR-9632823.

REFERENCES

1. Z.L. Wang and Z.C. Kang, Functional and Smart Materials - Structural Evolution and Structure Analysis, Plenum Press, New York, 1997.
2. C. Zener, Phys. Rev. **82**, 403 (1951).
3. R.F. Egerton, Electron Energy-Loss Spectroscopy in the Electron Microscope, 2nd ed., New York: Plenum Press, 1996.
4. J.H. Rask, B.A. Mine and P.R. Buseck, Ultramicroscopy **32**, 319 (1987).
5. D.H. Pearson, C.C. Ahn and B. Fultz, Phys. Rev. B **47**, 8471 (1993).
6. H. Kurata and C. Colliex, Phys. Rev. B **48**, 2102 (1993).
7. Z.L.Wang, J.S. Yin, Y.D. Jiang and J. Zhang, Appl. Phys. Lett. **70**, 3362 (1997).
8. Z.L. Wang and J.S. Yin, Phil. Mag. B, in press (1997).
9. J. Zhang, R.A. Gardiner, P.S. Kirlin, R.W. Boerstler and J. Steinbeck, Appl. Phys. Lett. **61**, 2884 (1992).
10. Z.L. Wang and J. Zhang, Phys. Rev. B **54**, 1153 (1996).
11. J.S. Yin and Z.L. Wang, Microscopy and Microanalysis 3, Suppl. **2**, 599 (1997).
12. J. Jin, T.H. Tiefel, M. McCormack, R.A. Fastnacht, R. Ramech and L.H. Chen, Science, **264**, 413 (1994).
13. R. Von Helmolt, J. Wecker, B. Holzapfel, L. Schultz and K. Samwer, Phys. Rev. Lett., **71**, 2331 (1994).
14. S.J. Lloyd, G.A. Botton and W.M. Stobbs, J. Microsc. **180**, 288 (1995).
15. J. Yuan, E. Gu, M. Gester, J.A.C. Bland and L.M. Brown, J. Appl. Phys. **75**, 6501 (1994).
16. Z.L. Wang, J.S. Yin, W.D. Mo and J.Z. Zhang, J. Phys. Chem. B 101 (No. 35), 6793 (1997).